Bratislava Medical Journal
https://doi.org/10.1007/s44411-026-00486-5

RESEARCH

Prenatal Exposure to Copper Sulfate: Effects on Fetal Development in Rats

Sümeyye Uçar[1] · Seher Yılmaz[2] · Şükrü Ateş[2] · Aslı Okan Oflamaz[3] · Züleyha Doğanyiğit[3] · Osman Öztürk[4] · Evrim Suna Arıkan Söylemez[5]

Received: 10 October 2025 / Revised: 17 December 2025 / Accepted: 4 January 2026
© The Author(s) 2026

Abstract

Copper sulfate is a pesticide widely used in Türkiye to treat bacterial and fungal infections on various fruit and nut trees. Despite its widespread use, insufficient data are available regarding its potential teratogenic and toxic effects during pregnancy. This study aimed to investigate the organ oxidative stress, immunohistochemistry, histopathology, and genetic effects of copper sulfate exposure in rat fetuses during pregnancy. Pregnant Wistar rats were administered 100 mg/kg copper sulfate daily via oral gavage throughout gestation. Fetuses were collected on day 21 of gestation and subjected to double skeletal staining to assess bone development. Additionally, fetal organ samples (liver, kidney, lung, brain, placenta, and heart) were analyzed histologically by Hematoxylin–Eosin (H&E) staining and immunohistochemically for inflammatory markers such as Tumor Necrosis Factor-Alpha (TNF-α), Nuclear Factor Kappa B (NF-κB), and Interleukin-6 (IL-6), and mRNA analysis was performed using real-time PCR for *TNF-α*, *IL-6*, and *NF-κB*. Oxidative stress was assessed using ELISA and biochemical assays for malondialdehyde (MDA), total antioxidant status (TAS), and total oxidant status (TOS). In the copper sulfate groups, compared to the control group, an increase in the number of degenerative glomeruli in the kidney and inflammatory cell infiltrations in the heart tissue, more frequent bleeding and cell infiltrations in the lungs, and an increase in the number of degenerative neurons in the brain and both giant trophoblast cells and glycogenic trophoblast cells in the placenta were observed. Immunohistochemical analyses revealed a significant increase in proinflammatory markers, including TNF-α, NF-κB, and IL-6, in fetal tissues in the copper sulfate-exposed group. Biochemical assessments showed a significant decrease in TAS and increases in MDA and TOS levels, indicating a marked oxidative stress state in all tissues examined. Furthermore, skeletal staining analyses revealed significant impairments in bone development in fetuses in the copper sulfate-exposed group compared to the control group. These findings suggest that prenatal copper sulfate exposure may cause significant histological damage, inflammatory responses, oxidative stress, and skeletal development in rat fetuses. Given the widespread use of copper sulfate in agriculture and the potential for human exposure, particularly among pregnant women in agricultural regions, further research is needed to reveal the full extent of its developmental toxicity.

Keywords Copper sulfate · Bone development · Double skeleton staining · Anatomy

✉ Sümeyye Uçar
sumeyyeucar@erciyes.edu.tr

Seher Yılmaz
seher.yilmaz@yobu.edu.tr

Şükrü Ateş
sukru.ates@yobu.edu.tr

Aslı Okan Oflamaz
asli.okan@bozok.edu.tr

Züleyha Doğanyiğit
zuleyha.doganyigit@gmail.com

Osman Öztürk
osman.ozturk@bozok.edu.tr

Evrim Suna Arıkan Söylemez
suna.arikan@afsu.edu.tr

[1] Department of Anatomy, Faculty of Medicine, Erciyes University, Kayseri, Turkey

[2] Present Address: Department of Anatomy, Faculty of Medicine, Yozgat Bozok University, Yozgat 66100, Turkey

[3] Department of Histology and Embryology, Faculty of Medicine, Yozgat Bozok University, 66100 Yozgat, Turkey

[4] Department of Pediatric Health and Diseases, Faculty of Medicine, Yozgat Bozok University, 66100 Yozgat, Turkey

[5] Department of Medical Biology, Faculty of Medicine, Afyonkarahisar Health Sciences University, Afyonkarahisar, Turkey

Published online: 22 January 2026

1 Introduciıon

Copper (Cu) is an necessary element found in trace amounts in both humans and animals. Besides act a part in iron funciton, Cu is also required for numerous biological processes, including antioxidant defense, neuropeptide synthesis, and immune function [1–3].

Cu is the primary active ingredient in various products, used in the forms of copper hydroxide, copper oxychloride, tribasic copper sulfate, and copper oxide [4]. But, Cu is most commonly used as a blend of copper sulfate and calcium hydroxide, a mixture referred to as "slaked lime" [5]. The resulting outcome acts as a fungicide and is called "Bordeaux mixture" [4, 5]. As a result of using this blend in vineyards, Cu levels in both the soil and the fruit are increased [6]. It is stated that in areas where pesticides were previously used heavily, copper and other pollutant metals can be determined at levels 50 times higher than in areas where pesticides were not used [4].

Excessive amounts of Cu lead to accumulation in various organs. Free Cu causes oxidative stress and, consequently, cell damage. Cu accumulation damages cells by producing free radical species that lead to oxidative stress [7–9].

Cu toxicity is considered the primary cause of organ damage in patients with Wilson disease (WD). Additionally, DNA damage, lipid peroxidation, and mitochondrial dysfunction are typically observed in the liver of WD patients. Morphological alters in hepatic mitochondria (containing widening of the interstitial space, separation of the inner and outer membranes, and formation of large vacuoles) typically take place in the early stages of WD and are considered a hallmark of hepatic damage in WD [10]. Cognitive dysfunction may accompany neurological deficits in patients with WD. Pathological changes in the basal ganglia appear to be the primary cause of this condition [10, 11].

The sensitivity of different organs to CuSO4 toxicity in rats was investigated at doses of 100 and 200 mg/kg for 30, 60 and 90 days, and it was concluded that the most affected organ by Cu toxicity was the liver, followed by the brain and kidneys [12]. Long-term (8 weeks by gavage) copper consumption (100 and 200 mg/kg) showed negative effects on the morphometric structure of the testes of rats from two weeks of age [13]. In a study investigating excitotoxicity, apoptosis, and astrocytic reactions in the hippocampus and frontal cortex and memory impairment, it was reported that copper toxicity (administered by gavage at a dose of 100 mg/kg for 30, 60, and 90 days) directly induces apoptosis and astrocytosis in the hippocampus and frontal cortex via glutamate and oxidative stress pathways, leading to impaired memory and learning [14]. Strong evidence was found that Cu toxicity can trigger autophagy and apoptosis via the mitochondrial pathway by inducing oxidative stress in rat kidneys (at doses of 30, 60, or 120 mg/kg for 6 months) [15].

Research in the literature has revealed no studies that comprehensively examine the effects of copper sulfate exposure during pregnancy on fetuses. Based on these studies, our aim was to examine organ damage in fetus histologically, bone development with double skeletal staining method, oxidative stress markers with ELISA, and TNF-α, NF-kB and IL-6 immunohistochemically in female rat fetuses exposed to copper sulfate during pregnancy.

2 Method

The ethical approval for this study was obtained by the Animal Care and Use Committee (Ethics Committee) of Erciyes University (Date:02.08.2023 and numbered 23/138). During this study, all procedures were carried out the following ethical issues. Experimental procedures were conducted in accordance with the guidelines for the care and use of laboratory animals in scientific research.

Sprague–Dawley female rats, 70–100 days old and weighing 250–300 g, obtained from Erciyes University DEKAM, were used for the study. The rats were fed a standard rat diet. Rats were housed together overnight between 5:00 PM and 8:00 AM with one adult male rat per cage to facilitate mating. After the males were removed, a vaginal smear was performed to confirm mating success. Female rats with sperm detected in the smear were considered to be pregnant for 0.5 days. The female rats with confirmed pregnancies were divided into two groups of five. They were subsequently housed for nine days in air-conditioned rooms, where the temperature was maintained at 21 °C. Food and

Table 1 Primer seguences of the related genes

Gene	Forward Primer 5' → 3'	Reverse Primer 5' → 3'
Rat-*TNF-α*	AAATGGGCTCCCTCTCATCAGTTC	TCTGCTTGGTGGTTTGCTACGAC
Rat-*IL-6*	TCCTACCCCAACTTCCAATGCTC	TTGGATGGTCTTGGTCCTTAGCC
Rat-*Nf-κB*	GCAAACCTGGGAATACTTCATGTGACTAAG	ATAGGCAAGGTCAGAATGCAC CAGAAGTCC
Rat-*GAPDH*	GAGGACCAGGTTGTCTCCTG	GGATGGAATTGTGAGGGAGA

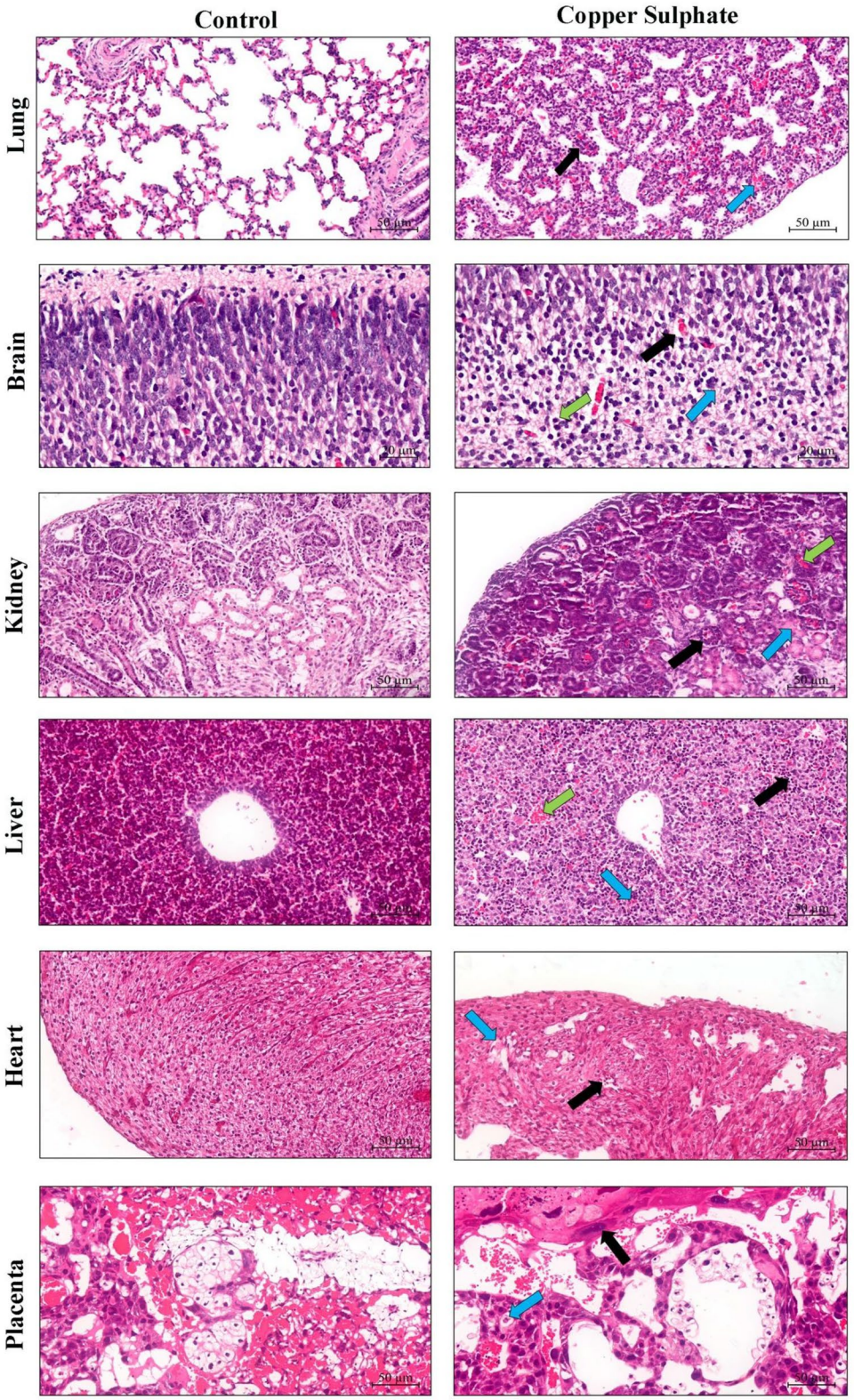


Fig. 1 Hematoxylin–eosin photomicrographs of lung, brain, kidney, liver, heart, and placenta tissues from the experimental groups. The black arrow in the lung images indicates alveolar wall thickening, and the blue arrow indicates hemorrhage. The black arrow in the brain images indicates perivascular edema, the blue arrow indicates satellitosis, and the green arrow indicates degenerative neurons. The black arrow in the kidney images indicates glomerular degeneration, the blue arrow indicates vacuolization, and the green arrow indicates hemorrhage. The black arrow in the liver images indicates inflammatory cell infiltration, the blue arrow indicates pyknotic hepatocytes, and the green arrow indicates hemorrhage. The black arrow in the heart images indicates cell infiltration, and the blue arrow indicates disarray of myocardial fibers. The black arrow in the placenta images indicates giant trophoblast cells, and the blue arrow indicates glycogenic trophoblast cells. Magnification in the lung, kidney, liver, heart, and placenta images is 20X, and the scale bar is 50 µm. Magnification in brain images is 40X and scale bar is 20 µm

water were available ad-libitum in a 12-h light and 12-h dark environment.

The choice of experimental dose was based on previous toxicological studies and 100 mg/kg copper II sulphate pentahydrate (purity > 98.0%,CAS number: 7758-99-8, purchased from Isolab chemicals, Germany)[14] was added to the standard diet via gavage of the experimental group, while the control group received physiological saline. Copper

Table 2 Histopathological damage rates in liver tissues of experimental groups

Groups	Pycnotic hepatocytes	Hemorrhage	Inflammatory cell infiltration
Control	1 ± 0.45	0.2 ± 0.45	0.6 ± 0.55
Copper Sulphate	2.4 ± 0.55***	2 ± 0.89***	2.2 ± 0.71**

Statistically, data obtained from the groups were compared using an independent t-test. Data shown in the table are expressed as mean SD. ***p = 0.0003, **p = 0.0016 indicate a statistically significant difference compared to the control group

Table 3 Histopathological damage rates in kidney tissues of the experimental groups

Groups	Tubulointerstitial Damage Lesions			Glomerular Degeneration
	Vacuolization	Hemorrhage	Infiltration of inflammatory cells	
Control	1.2 ± 0.71	0.2 ± 0.45	1 ± 0.45	0.8 ± 0.89
Copper Sulphate	2.4 ± 0.55*	1.4 ± 0.45*	2.2 ± 0.55**	2.4 ± 0.55**

Statistically, data obtained from the groups were compared using an independent t-test. Data shown in the table are expressed as mean SD. **p = 0.002, *p < 0.05 indicates a statistically significant difference compared to the control group

Table 4 Histopathological damage rates in heart tissues of the experimental groups

Groups	Inflammatory cell infiltration	Myocardial fiber disorganization
Control	0.4 ± 0.54	0.4 ± 0.55
Copper Sulphate	1.8 ± 0.45*	2 ± 0.89***

Data obtained from the groups were compared statistically using an independent t-test. Data shown in the table are expressed as mean SD. *** p = 0.0001, *p < 0.05 indicates a statistically significant difference compared to the control group

Table 5 Histopathological damage rates in lung tissues of the experimental groups

Groups	Hemorrhage	Cellular Infiltration	Alveolar wall thickening
Control	1 ± 0.54	0.6 ± 0.55	0.2 ± 0.45
Copper Sulphate	2.6 ± 0.45**	2 ± 0.89**	2.2 ± 0.79**

Data obtained from the groups were compared statistically using an independent t-test. Data shown in the table are expressed as mean SD. *** *p = 0.0001*, ** *p < 0.01* indicates a statistically significant difference compared to the control group

Table 6 Histopathological damage rates in brain tissues from experimental groups

Groups	Degenerative neurons	Satellitosis	Perivascular edema
Control	1.2 ± 0.45	0.6 ± 0.55	1 ± 0.45
Copper Sulphate	2.4 ± 0.55**	2 ± 0.89**	2.2 ± 0.55**

Data obtained from the groups were compared statistically using an independent t-test. Data shown in the table are expressed as mean SD. *** *p = 0.0001*, ** *p < 0.01* indicates a statistically significant difference compared to the control group

Table 7 Histopathological damage rates in placental tissues of experimental groups

Groups	Giant trophoblast cells	Glycogenic trophoblast cells
Control	0.4 ± 0.55	0.2 ± 0.45
Copper Sulphate	2.2 ± 0.45***	2.2 ± 0.84**

Data obtained from the groups were compared statistically using an independent t-test. Data shown in the table are expressed as mean SD. *** *p = 0.0001*, ** *p < 0.01* indicates a statistically significant difference compared to the control group

sulfate was added to the diet by gavage. Copper sulfate was dissolved in physiological saline at a dose of 100 mg/kg and given to pregnant rats by gavage. Copper sulfate was easily dissolved in physiological serum. The mixture was homogenized by vortexing.Copper sulfate and saline were administered to both groups, respectively, from days 6–15 of pregnancy, which includes the organogenesis period, the most sensitive period to drugs and teratogens. All rats were sacrificed on day 21 of pregnancy, and tissues were collected from fetuses(litters). At the end of the 21st day, the fetuses of the pregnant rats were removed by caesarean section under ketamine-xylazine anesthesia. After removal, the fetuses were sacrificed by cervical dislocation.

Control Group (Pregnant female rats, n = 5): Rats in the control group received physiological saline in addition to a standard rat diet. Pregnant rats were administered physiological saline for 21 days, and analyses were performed on offspring (pups n = 50) collected at the end of day 21.

Copper sulfate Group (Pregnant female rats, n = 5): This group received copper sulfate at a dose of 100 mg/kg/day in addition to a standard rat diet throughout pregnancy [16] Each rat was administered copper sulfate via gavage, feeding equal doses. Pregnant rats in the copper sulfate group were administered copper sulfate via gavage for 21 days, and analyses were performed on offspring (pups n = 50) collected at the end of day 21.

Tissue samples taken at the end of the experiment were first fixed in a 10% formaldehyde solution. After fixation, the tissues were dehydrated by passing through ascending alcohol series (50%, 70%, 80%, 96%, 100%). The tissues, cleared with xylene, were embedded in paraffin, and 5 µm-thick sections were cut from the blocks. Histopathological changes in the tissues (cell shape, morphology, number, edema, etc.) were determined under a light microscope using Hematoxylin–Eosin (H-E) staining [25]. Liver, kidney, lung, brain, placenta and heart tissues were examined with histopathological analysis using Hematoxylin–eosin staining, immunohistochemical and PCR analysis using TNF-α, NF-kB and IL-6 [25], and oxidative stress markers MDA, TAS and TOS were analyzed using ELISA [42], and bone development was examined with double skeletal staining [25, 40].

2.1 Histological Analysis (Fetuses n = 10)

Lung, brain, kidney, liver, heart, and placental tissues were fixed with 10% formaldehyde solution and then washed in tap water (overnight). Tissue dehydration was performed through an ascending alcohol series (70%, 80%, 90%, and 100%), followed by clearing in Xylol (1,082,984,000, Merck) and paraffin embedding. From the paraffin blocks, 5-µm-thick sections were obtained using a microtome, stained with Harris hematoxylin and eosin, examined under a light microscope (Zeiss Axiscope 3), and imaged with a Colibri 3 digital camera. Histopathological evaluation focused on tissue-specific lesion profiles: hepatocellular injury (hollow and pyknotic hepatocytes), hemorrhage, and inflammatory infiltration within venules and sinusoids in the liver [17].; glomerular degeneration and tubulointerstitial alterations (vacuolization, hemorrhage, inflammatory infiltration) in the kidney [18]; myocardial fiber disorganization and inflammatory infiltration in the heart [19, 20]; alveolar wall thickening, hemorrhage, and cellular infiltration in the lung [21]; neuronal degeneration, satellitosis, and perivascular edema in the brain [22]; and giant and glycogenic trophoblast cells in placental tissue [23]. All parameters were scored on a four-point scale (0 = absent, 1 = mild, 2 = moderate, 3 = severe). Quantification was performed in randomly selected fields by two independent investigators blinded to the experimental groups.

2.2 Immunohistochemical Analysis(Fetuses n = 10)

Immunohistochemical analysis was performed using the Avidin–Biotin peroxidase method to detect immunoreactivity for anti-IL-6 (E-AB-30095, Elabscience), anti-NF-kB (BT-MCA1291, Bioassay Technology Laboratory), and anti-TNF-α (E-AB-22159, Elabscience) in sections taken from lung, brain, kidney, liver, heart, and placental tissues of the experimental groups [24]. Briefly, after deparaffinization of 5 µm-thick sections, citrate buffer (pH: 6.0; Thermo Fischer Scientific, UK, AP-9003–500) was used to reveal epitopes. Slides were then placed in a 3% hydrogen peroxide in methanol solution to prevent endogenous peroxidase activity. Ultra V blocking solution (Thermo Fischer Scientific, UK, TA-125-UB) was applied to prevent nonspecific staining. The slides were then incubated overnight at 4 °C with primary antibodies (diluted IL-6 1:100, NF-kB 1:50, TNF-α 1:100). Subsequently, the slides were incubated with biotinylated goat anti-polyvalent secondary antibody (Thermo Fischer Scientific, UK, TP-125-BN) for 40 min at room temperature. After several washes with PBS, the samples were incubated with streptavidin peroxidase (Thermo Fischer Scientific, UK, TS-125-HR) for 30 min at room temperature. The antibody complex was visualized by incubation with diaminobenzidine (DAB) chromogen (Thermo Fischer Scientific, UK, TA-125-HD). Sections were then counterstained with Gill III Hematoxylin (Merck, Germany, 1.05174.1000). They were dehydrated by passing through an ascending alcohol series and coverslipped with entellan. Sections were examined with a Zeiss Axiscope 3 light microscope and imaged with a Colibri 3 digital camera.

2.3 ELISA Analysis (Fetuses n = 10)

The MDA kit (SunRed Biological Technology Cat. No: 201-11-0157) was used to measure malondialdehyde levels in tissues. Measurements were made using a spectrometer (BMG LabTech SPECTROSTAR Nano) at a wavelength of 450 nm, in accordance with the kit protocol. Data obtained are expressed in nmol/mL.

The TAS (Total Antioxidant Status) kit (Rel Assay Diagnostics, Turkey, REF No: RL0017, LOT No: JE 14042A) was used to measure total antioxidant levels. Measurements were made using a spectrometer (BMG LabTech SPECTROSTAR Nano) at a wavelength of 660 nm, in accordance with the kit protocol. Data obtained are expressed in nmol/mL.

To measure total oxidant levels, the TOS (Total Oxidant Status) kit (Rel Assay Diagnostics, Turkey, REF No:

RL0024, LOT No: JE 14048Og) was used, and measurements were made with a spectrometer (BMG LabTech SPECTROSTAR Nano) at a wavelength of 530 nm according to the kit protocol. Data obtained are expressed in nmol/mL.

2.4 Dual Skeletal Staining (Fetuses n = 10)

To stain the fetal skeletal system using the double skeleton staining method, the method from our previous study was used [25].

2.5 Genetic Analysis (Fetuses n = 10)

Total RNA from the lung, brain, kidney, liver, heart and placenta tissues of the rats were extracted with PureZole reagent (Biorad, USA) according to the manufacturer's protocol. RNA amount and purity were quantified for each RNA sample by Nanodrop ND-1000 spectrophotometer V3.7. RNA samples were stored at -80 °C until use. All the RNA samples were reverse transcribed into cDNA from 1 µg of total RNA (iScript Reverse Trancription Supermix Biorad, USA). *TNF-α, IL-6* and *Nf-kB* mRNA expression analysis performed by Real-time PCR method using the Step-One-Plus Thermocycler (Applied Biosystems). Amplifications were performed in a total reaction volume of 20 µL using cDNA, site-specific primers (Oligomer Biyotechnology, Ankara), SsoAdvanced Universal Inhibitor-Tolerant SYBR Green Supermix (Biorad, USA) and nuclease-free water. *GAPDH* was used as internal controls. Primer sequences were designed as mentioned in [26] for *TNF*-α and *IL*-6, and was designed as mentioned in [27] for *Nf-κB* (Table 1):

2.6 Statistical Analysis

GraphPad Prism 10 was used for statistical analysis of experimental data. Immunoreactivity levels were assessed using ImageJ software. Histopathological evaluations were analyzed using an independent t-test. Numerical data obtained from immunohistochemical analysis were analyzed using independent t-tests and Shapiro–Wilk and Levene's tests. $P < 0.05$ was considered statistically significant. For Genetic analysis data analyzes were performed using REST 2009 V2.0.13 where $P < 0,05$ is deemed to represent a statistically significant result [28].

3 Results

3.1 Histological Results

More hepatocytes with pyknotic nuclei and significantly increased hemorrhage were observed in the liver tissues of the copper sulfate groups compared to the control groups. Furthermore, an increase in inflammatory cells was observed in the liver tissues of the copper sulfate group (Fig. 1, Table 2).

In the kidney tissues of the copper sulfate groups, inflammatory cells were found in the tubulointerstitial areas, increased tubular vacuolization, and an increased number of degenerated glomeruli compared to the control groups (Fig. 1, Table 3).

In the heart tissues of the copper sulfate groups, an increase in the number of inflammatory cell infiltrations and more disorganized myocardial fibers were observed compared to the control groups (Fig. 1, Table 4).

When lung tissue was examined, hemorrhage, cellular infiltration, and alveolar wall thickening were observed more frequently in the tissues of the copper sulfate group compared to the control group (Fig. 1, Table 5).

When the prefrontal cortex area of the brain was examined, an increase in the number of degenerative neurons, satellite disease and perivascular edema were observed in the tissues of the copper sulfate group compared to the control group (Fig. 1, Table 6).

In placental tissues taken from mothers of fetuses in the copper sulfate groups, an increase in both giant trophoblast cells and glycogenic trophoblast cells was observed compared to the control groups (Fig. 1, Table 7).

3.2 Immunohistochemistry Findings

NF-kB expression was observed to be statistically significantly increased in the lung, kidney, heart, and placental tissues of the copper sulfate groups compared to the control groups, while no statistically significant difference was observed in the brain and liver tissues ($p < 0.05$, Fig. 2).

When TNF-κB expression was evaluated, it was observed that TNF-κB expression was statistically significantly increased in the lung, brain, kidney, liver, and heart tissues of the copper sulfate groups compared to the control groups, while no statistically significant difference was observed in the placental tissue ($p < 0.05$, Fig. 3).

IL-6 expression levels were observed to be higher in the lung, brain, liver, heart, and placental tissues of the copper sulfate groups compared to the control groups ($p < 0.05$). When the kidney tissues of the copper sulfate and control groups were compared, no statistically significant difference was observed ($p < 0.05$, Fig. 4).

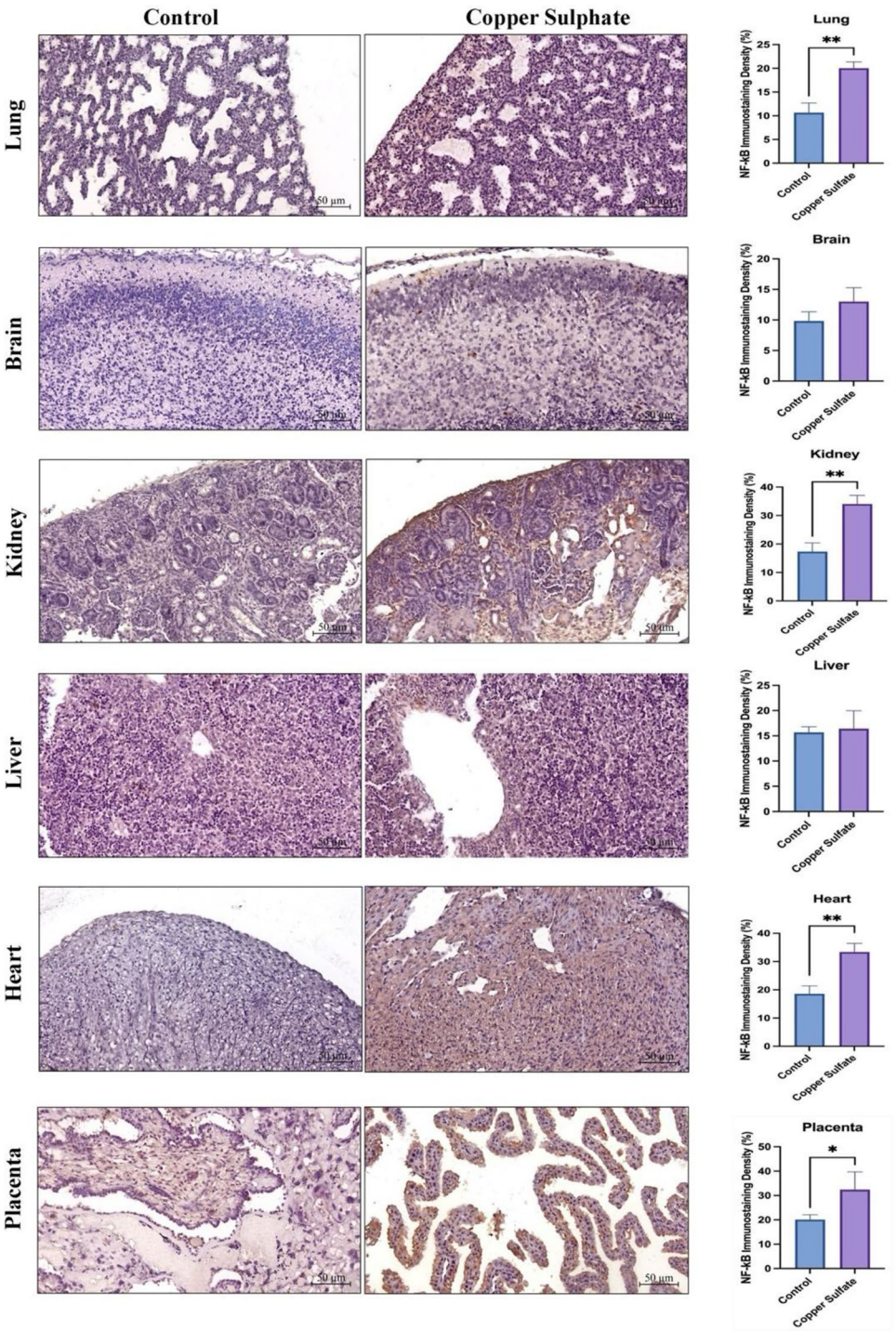


Fig. 2 NF-kB staining images in lung, brain, kidney, liver, heart, and placenta tissues of the experimental groups. Data shown in the graph are expressed as mean SD. Statistical comparisons were made using independent t-tests and Shapiro–Wilk-Levene tests. *$p < 0.05$ and **$p < 0.01$ indicate a significant difference between the control and copper sulfate groups. Magnification is 20X, and the scale bar is 50 µm

3.3 ELISA Findings

MDA concentration levels were observed to be significantly higher in the lung, brain, kidney, liver, and placenta tissues of the copper sulfate groups compared to the control groups. However, no significant difference was observed in the heart tissue ($p < 0.05$, Fig. 5). TAS concentration levels were observed to be significantly lower in all tissues of the copper sulfate groups compared to the control groups ($p < 0.05$, Fig. 6). TOS concentration levels were observed to be significantly higher in all tissues of the copper sulfate groups compared to the control groups ($p < 0.05$, Fig. 7).

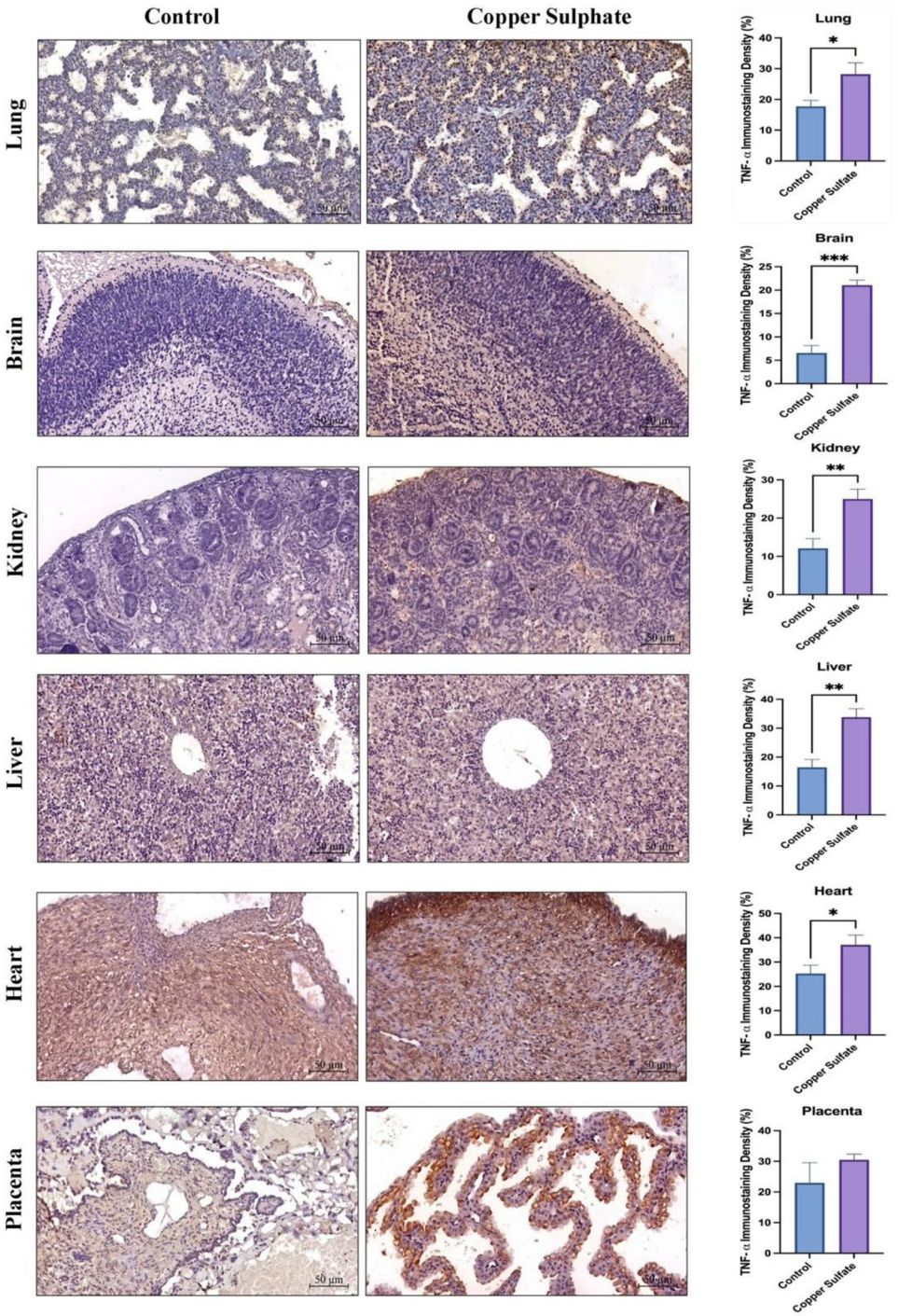


Fig. 3 TNF-staining images in lung, brain, kidney, liver, heart, and placenta tissues of the experimental groups. Data shown in the graph are expressed as mean SD. Statistical comparisons were made using independent t-tests and Shapiro–Wilk-Levene tests. $*p < 0.05$, $**p < 0.01$, and $***p < 0.001$ are statistically significant. Magnification is 20X, and the scale bar is 50 µm

3.4 Double Skeletal Staining Findings

Following the double skeletal staining procedure, the fetuses were photographed and measured. Data for total length, total area, bone length, and bone area of the fore and hind limb bones were obtained.

Data analysis revealed that fetus and placenta weights decreased significantly in the copper sulfate group compared to the control group. While no significant difference was observed in the head-rump length, biparietal and occipito-frontal length values were found to be significantly lower than the copper values compared to the control group (Table 8).

In the copper sulfate group, right Total length, total area, bone length, and bone area values of the scapula were observed to be importantly lower than those in the control group. A statistically important decrease was detected in the total length, total area, bone length, and bone area values of

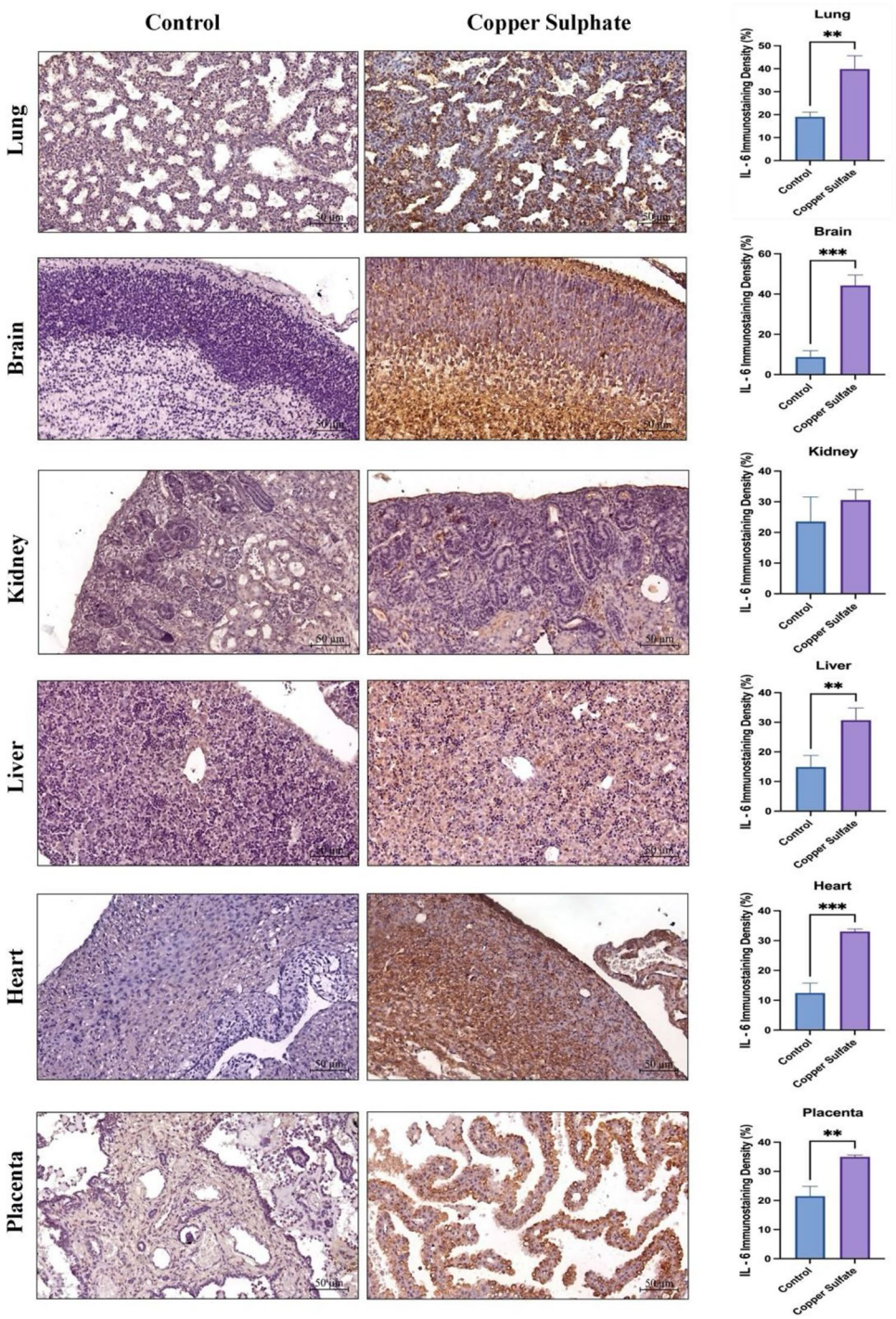


Fig. 4 IL-6 staining images in lung, brain, kidney, liver, heart, and placenta tissues of the experimental groups. Data shown in the graph are expressed as mean SD. Statistically, data obtained from the groups were compared using independent t-tests and Shapiro–Wilk-Levene tests. $^{**}p < 0.01$ and $^{***}p < 0.001$ are statistically significant. Magnification is 20X, and the scale bar is 50 µm

the humerus, radius, and ulna bones in the copper sulfate group compared to the control group (Table 9, Fig. 8).

Statistically significant decreases were detected in the total length, total area, bone length, and bone area values of the right femur, tibia, and fibula in the copper sulfate group compared to the control group (Table 9, Fig. 8).

The total length, total area, bone length, and bone area values of the left scapula were observed to be importantly lower in the copper sulfate group compared to the control group. Statistically significant decreases were detected in the total length, total area, bone length, and bone area values of the humerus, radius, and ulna in the copper sulfate group compared to the control group (Table 10, Fig. 9).

Statistically significant decreases were detected in the total length, total area, bone length, and bone area values of

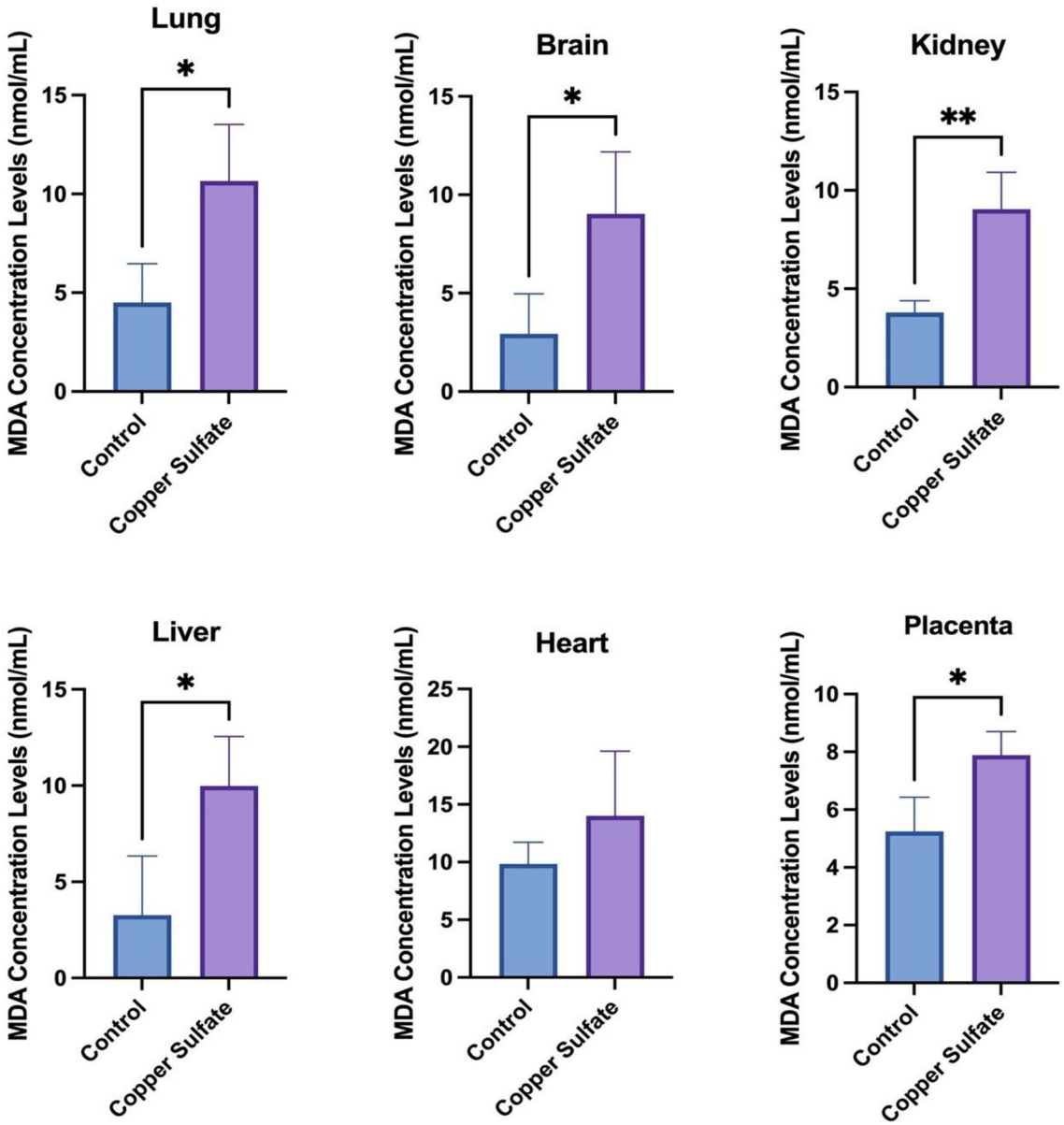


Fig. 5 MDA concentration levels in the lung, brain, kidney, liver, heart, and placenta tissues of the experimental groups. Statistically, data for the lung, brain, kidney, liver, heart, and placenta tissues obtained from the groups were compared using independent t-test and Shapiro–Wilk-Levene's tests. $*p < 0.05$ and $**p < 0.01$ indicate a significant difference between the control and copper sulfate groups

the left femur, tibia, and fibula in the copper sulfate group compared to the control group (Table 10, Fig. 9).

3.5 mRNA Analysis of *TNF-α, IL-6 and Nf-κB*

The mRNA levels of the ***TNFα*** gene were changed in lung (0.63 fold change), in brain (2.31 fold change, $*P < 0.001$), in kidneys (0.33 fold change), in liver (0.91 fold change), in heart (0.247 fold change) and in placenta (5.72 fold change, $*P < 0.001$) compared to mRNA levels of related control tissues (Fig. 10). The mRNA levels of the ***IL-6*** gene were changed in lung (0.89 fold change), in brain (2.5 fold change), in kidneys (0.48 fold change), in liver (2.42 fold change), in heart (2.71 fold change) and in placenta (9.2 fold change, $*P < 0.001$) compared to mRNA levels of related control tissues (Fig. 10).The mRNA levels of the *Nf-κB* gene were changed in lung (1.65 fold change), in brain (0.47 fold change), in kidneys (0.23 fold change), in liver (0.72 fold change), in heart (1.67 fold change) and in placenta (1.26 fold change, $*P < 0.001$) compared to mRNA levels of related control tissues (Fig. 10).

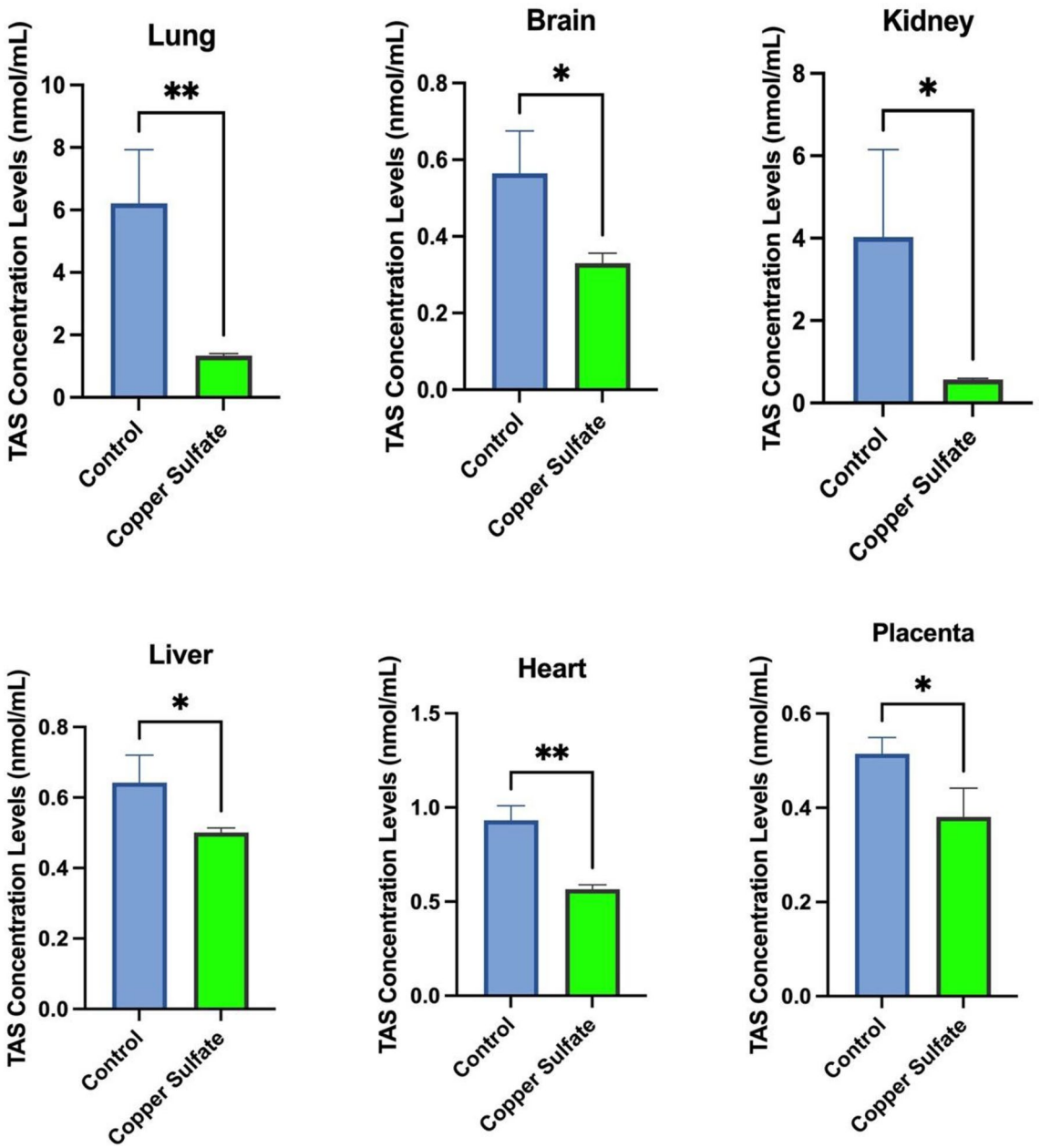


Fig. 6 TAS concentration levels in the lung, brain, kidney, liver, heart, and placenta tissues of the experimental groups. Statistically, data for the lung, brain, kidney, liver, heart, and placenta tissues obtained from the groups were compared using independent t-test and Shapiro–Wilk-Levene's tests.*$p < 0.05$ and **$p < 0.01$ indicate a significant difference between the control and copper sulfate groups

4 Discussion and Conclusion

Copper sulfate is a widely used pesticide. Pesticides are degraded and eliminated very slowly by biological, chemical, and physical processes in the natural environment. This makes their effects on humans more likely to be seen through food, water, and soil. In mammals, Cu is ingested in the diet and, after being taken into cells from intestinal epithelial cells by CTR1, reaches the liver via the portal circulation. The liver is the main reservoir of Cu in the body and controls its distribution to peripheral organs via the bloodstream or its excretion via the bile. When the amount of Cu within the cell is too high to be stored, it is removed from the body via the bile [29]. Copper is maintained at a certain level within the cell through these pathways. An increase in the amount of free Cu within the cell causes cytotoxicity due to oxidative stress [9].

Cu toxicity leads to significant oxidative stress and subsequent tissue damage. The oxidative stress associated with Cu toxicity is, in part, a result of redox reactivity; for example,

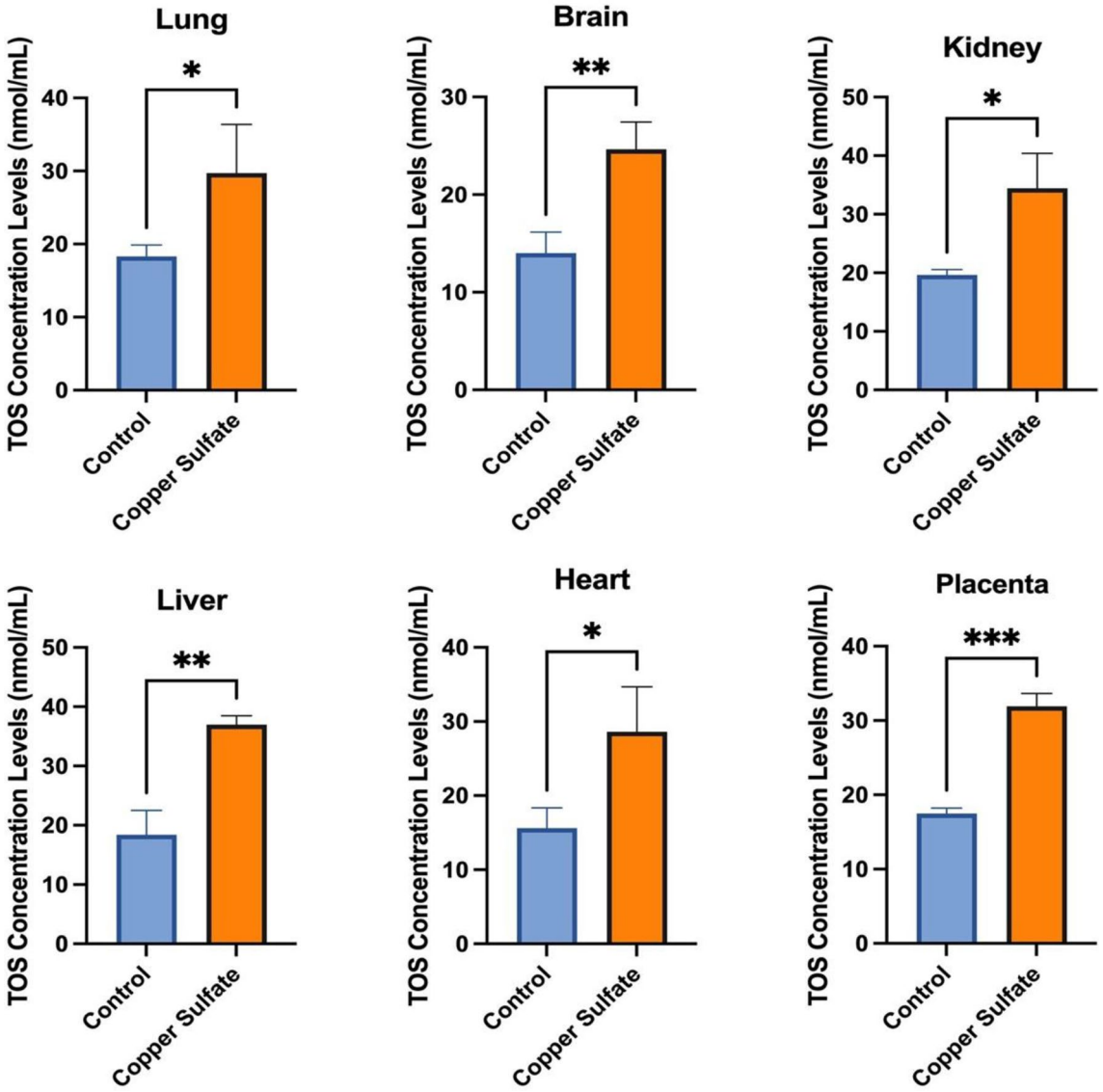


Fig. 7 TOS concentration levels in the lung, brain, kidney, liver, heart, and placenta tissues of the experimental groups. Statistically, data for the lung, brain, kidney, liver, heart, and placenta tissues obtained from the groups were compared using independent t-test and Shapiro–Wilk-Levene's tests. *$p<0.05$ and **$p<0.01$ and ***$p=0.0001$ indicate a significant difference between the control and copper sulfate groups

free Cu or low-molecular-weight Cu complexes catalyze the reaction between superoxide anion and H2O2 to produce the hydroxyl radical [30].

Table 8 Fetus and placenta weights and length measurements

Parameter	Control	Copper sulfate	*p*
Fetus weight	2.29 ± 0.16	1.90 ± 0.09*	< 0,0001
Plecental weight	0.58 ± 0.07	0.45 ± 0.03*	< 0,0001
Fore–aft length	26.87 ± 1.88	25.36 ± 2.24	0,1200
Biparietal length	7.44 ± 0.24	7.03 ± 0.13*	0,0002
Occipitofrontal length	8.31 ± 0.69	7.67 ± 0.15*	0.01

The AMPK-mTOR pathway in GC-1 cells and testes in response to oxidative stress under CuSO4 was investigated, and copper sulfate can induce autophagy via the AMPK-mTOR pathway, downregulating p-mTOR/mTOR and subsequently upregulating p-AMPKα/AMPKα and p-ULK1/ULK1 [43]. It has also been found that copper exposure activates double-stranded RNA-dependent protein kinase (PKR), as evidenced by an increase in the ratio of phosphorylated PKR and total PKR at Thr451, and increases the phosphorylation of the downstream signaling molecule eukaryotic initiation factor 2α (eIF2α) at Ser51 in the hippocampus [44]. The endoplasmic reticulum (ER) is a toxicological target in copper poisoning. CuSO4-induced ER stress

Table 9 Length and area measurements in the right fore and hind extremity bones

Bone (right)	Parameter	Control	Copper sulfate	*p*
Scapula	Total length	4.82 ± 0.09	4.08 ± 0.13*	< 0.000001
	Total area	5.40 ± 0.37	4.72 ± 0.39*	0.000727
	Bone length	2.42 ± 0.06	2.18 ± 0.23*	0.004642
	Bone area	2.37 ± 0.09	2.19 ± 0.15*	0.005791
Humerus	Total length	5.03 ± 0.17	4.71 ± 0.071*	< 0.0001
	Total area	5.87 ± 0.21	4.95 ± 0.41*	< 0.0001
	Bone length	2.61 ± 0.12	2.34 ± 0.15*	0.000284
	Bone area	2.93 ± 0.08	2.55 ± 0.29*	0.000832
Radius	Total length	3.75 ± 0.14	3.45 ± 0.32*	0.013211
	Total area	2.06 ± 0.16	1.75 ± 0.12*	0.000118
	Bone length	2.54 ± 0.16	2.22 ± 0.14*	0.000171
	Bone area	1.04 ± 0.07	0.9 ± 0.11*	0.002930
Ulna	Total length	4.94 ± 0.18	4.52 ± 0.23*	0.000234
	Total area	2.92 ± 0.35	2.59 ± 0.09*	0.012554
	Bone length	2.75 ± 0.17	2.51 ± 0.14*	0.003656
	Bone area	1.46 ± 0.17	1.28 ± 0.09*	0.006820
Femur	Total length	4.59 ± 0.39	3.99 ± 0.08*	0.000163
	Total area	4.61 ± 0.53	3.55 ± 0.10*	0.000008
	Bone length	2.03 ± 0.12	1.77 ± 0.08*	0.000017
	Bone area	1.59 ± 0.34	1.35 ± 0.07*	0.035517
Tibia	Total length	3.78 ± 0.43	3.39 ± 0.11*	0.011711
	Total area	2.81 ± 0.39	2.12 ± 0.03*	0.000028
	Bone length	2.37 ± 0.24	1.99 ± 0.06*	0.000171
	Bone area	1.54 ± 0.34	1.15 ± 0.05*	0.001999
Fibula	Total length	3.88 ± 0.51	3.50 ± 0.09*	0.036222
	Total area	1.79 ± 0.27	1.35 ± 0.09*	0.000113
	Bone length	2.17 ± 0.10	1.67 ± 0.11*	< 0.000001
	Bone area	0.81 ± 0.13	0.55 ± 0.09*	0.000054

promoted hepatic apoptosis in mice by activating the CHOP, JNK, and caspase-12 signaling pathways [45].

Luo et al., examined the toxic effects of copper nanoparticles (Cu NPs), which have been shown to cross the placental barrier, on fetuses in pregnant rats and reported their effects on fetuses. Oral exposure to Cu NPs during pregnancy increased fetal Cu levels, which not only affected fetal development but also significantly triggered oxidative stress and inflammatory responses in the fetal liver [31]. Lee et al. compared copper nanoparticles (Cu NPs) and copper microparticles (Cu MPs, 14–25 μm) administered orally to Sprague–Dawley rats at doses of 0, 100, 200 and 400 mg/kg/day for 28 days in vivo. The results showed that Cu NPs caused damage to red blood cells, thymus, spleen, liver and kidney [32].

Copper accumulation or depletion can alter neuronal function and lead to neuronal degeneration and brain dysfunction. The effects of high copper intake on the cerebellum have been investigated. A significant decrease in the total volume of cerebellar structures was observed in Cu-treated rats. Total cell numbers in the cerebellar cortex and deep cerebellar nuclei were significantly reduced in a dose-dependent manner by Cu. These changes resulted in motor performance impairments in the animals [38].

A study evaluating the extent of apoptosis and glial activation in the corpus striatum following Cu toxicity in a rat model found that total distance traveled, movement time, number of upright postures, latency to fall on a rotarod, and grip strength decreased, and rest time increased in the group administered orally with copper sulfate. Impaired locomotor activity in rats with Cu toxicity was reported to be associated with apoptotic and inflammatory-mediated cell death in the corpus striatum due to Cu-mediated oxidative stress and excitotoxicity [35].

In our study, fetuses exposed to copper sulfate for 21 days showed an increase in hepatocytes with pyknotic nuclei, hemorrhage, and inflammatory cells in their livers. Inflammatory cells, increased tubular vacuolization, and an increased number of degenerated glomeruli were detected in the tubulointerstitial spaces of the kidney tissue. In the copper sulfate group, inflammatory cell infiltration in the heart tissue and an increase in irregular myocardial fibers were observed. Hemorrhage, cellular infiltration, and alveolar wall thickening were observed in the lungs. The number

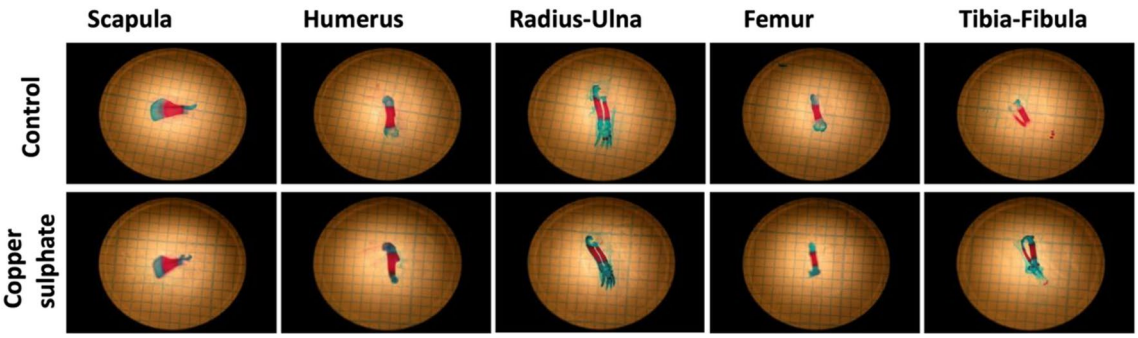


Fig. 8 Staining images of the right upper and lower extremity bones for the control and copper sulfate groups

Table 10 Length and area measurements in the left fore and hind extremity bones

Bone (left)	Parameter	Control	Copper sulfate	*p*
Scapula	Total length	4.85 ± 0.09	4.07 ± 0.13*	< 0.000001
	Total area	5.71 ± 0.49	4.80 ± 0.41*	0.000314
	Bone length	2.44 ± 0.11	2.18 ± 0.23*	0.006192
	Bone area	2.36 ± 0.05	2.19 ± 0.15*	0.005225
Humerus	Total length	5.02 ± 0.14	4.73 ± 0.09*	0.000035
	Total area	5.79 ± 0.39	4.98 ± 0.42*	0.000260
	Bone length	2.61 ± 0.12	2.31 ± 0.17*	0.000216
	Bone area	2.89 ± 0.13	2.59 ± 0.26*	0.004583
Radius	Total length	3.73 ± 0.14	3.45 ± 0.30*	0.014834
	Total area	2.05 ± 0.21	1.76 ± 0.11*	0.001238
	Bone length	2.53 ± 0.12	2.23 ± 0.14*	0.000070
	Bone area	1.04 ± 0.07	0.89 ± 0.10*	0.001642
Ulna	Total length	4.91 ± 0.20	4.51 ± 0.23*	0.000725
	Total area	3.01 ± 0.49	2.58 ± 0.09*	0.013874
	Bone length	2.81 ± 0.16	2.50 ± 0.15*	0.000317
	Bone area	0.46 ± 0.16	1.28 ± 0.10*	0.009047
Femur	Total length	4.51 ± 0.21	4.02 ± 0.09*	0.000002
	Total area	4.33 ± 0.28	3.55 ± 0.11*	< 0.000001
	Bone length	1.96 ± 0.12	1.76 ± 0.09*	0.000410
	Bone area	1.45 ± 0.13	1.35 ± 0.07*	0.037533
Tibia	Total length	3.75 ± 0.21	3.38 ± 0.11*	0.000125
	Total area	2.65 ± 0.18	2.14 ± 0.03*	< 0.000001
	Bone length	2.3 ± 0.29	0.99 ± 0.07*	0.004254
	Bone area	1.48 ± 0.26	1.13 ± 0.04*	0.000489
Fibula	Total length	3.73 ± 0.17	3.51 ± 0.08 *	0.001218
	Total area	1.78 ± 0.24	1.34 ± 0.10*	0.000054
	Bone length	2.15 ± 0.17	1.64 ± 0.12*	< 0.000001
	Bone area	0.79 ± 0.13	0.52 ± 0.09*	0.000036

of degenerative neurons in the brain, satellite disease, and perivascular edema have increased. An increase in both giant trophoblast cells and glycogenic trophoblast cells was also observed in the placenta.

In a study, the effects of copper sulfate (CuSO4) on rat spermatogenesis were investigated. Rats were administered CuSO4 via gavage at doses of 0, 100, 200, and 400 mg/kg for 30 days. Results showed that testicular coefficients, sperm count, testosterone (T), luteinizing hormone (LH), and follicle-stimulating hormone (FSH) concentrations, as well as glutathione peroxidase (GSH-Px) and superoxide dismutase (SOD) activities, were decreased in the CuSO4-treated groups, while the rate of abnormal malformations and malondialdehyde (MDA) concentrations were increased compared to the control group. This suggests that CuSO4 exposure impairs sperm quality, suppresses rat spermatogenesis by inhibiting sex hormone and gonadotropin secretion and testicular antioxidant function [16]. The study revealed that exposure to high Cu concentrations may cause oxidative stress-induced liver damage by increasing the hepatic function index (ALT, AST, and ALP) and MDA content, while decreasing the activity of oxidative stress-related antioxidant enzymes (T-SOD, GSH-Px, and CAT). The results showed that an appropriate dose of copper can improve liver function by promoting mitophagy and Cu enzymes, which play an antioxidant role, while excessive Cu accumulation can cause liver lesions by increasing apoptosis and inhibiting mitophagy pathways [37]. In one study, superoxide dismutase (SOD) activities, malondialdehyde (MDA) levels, and glutathione (GSH) concentrations were determined The brain MDA levels were found to be significantly higher in the experimental group than in the control group [41].

In our study, the MDA copper sulfate group showed increased activity in all tissues; the data are consistent with previous studies. ELISA results revealed that MDA and TOS concentrations were higher in the copper sulfate groups compared to the control groups, while TAS concentrations were significantly lower in all tissues of the copper sulfate groups compared to the control groups.

The effects of curcumin against copper sulfate (CuSO4)-induced hepatotoxicity were investigated, and curcumin treatment resulted in decreased levels of glutathione (GSH)

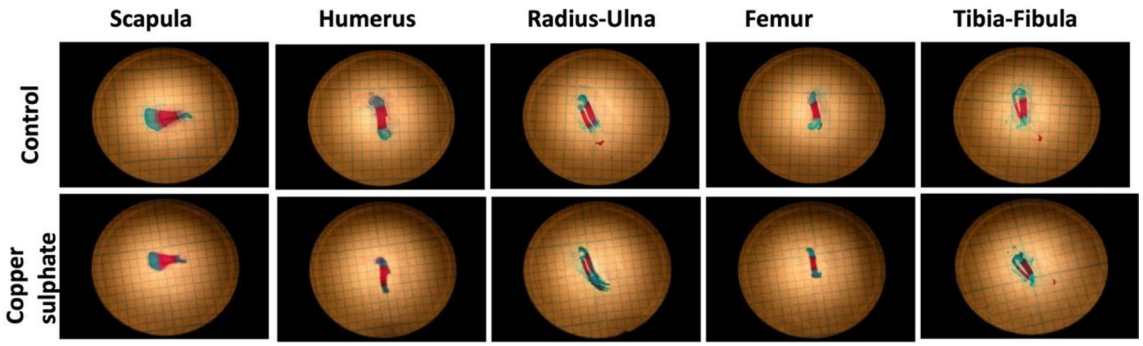


Fig. 9 Staining images of the left upper and lower extremity bones for the control and copper sulfate groups

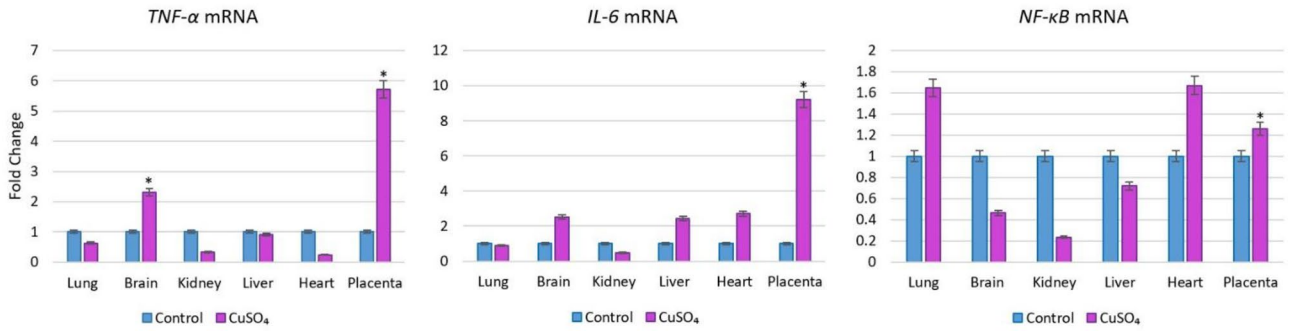


Fig. 10 The results of real-time PCR analysis. Relative mRNA expression of *TNFα, IL-6 and Nf-κB* gene in lung, brain, kidney, liver, heart and placenta tissues in rat fetuses exposed to Cu + + were given as fold change compared to the related controls. *Represents the significance of $P < 0.001$ compared to control. *GAPDH* is reference gene for normalization

and superoxide dismutase (SOD). Histopathological examinations confirmed these results [33].

Another study used resveratrol, an antioxidant compound, to combat Cu toxicity. Resveratrol mitigated the toxic effects of CuSO4 on the liver in rats, suggesting that resveratrol mitigates CuSO4-induced liver damage by reducing liver transaminase concentrations and oxidative stress, supporting antioxidant activity and cytochrome P450 enzymes, and maintaining a balance in trace element concentrations [34].

The protective role of rutin administration against Cu toxicity in Cu-induced brain damage was investigated. Cu administration increased malondialdehyde, nitric oxide levels, and myeloperoxidase activity in rat brains and decreased superoxide dismutase and catalase activities. Furthermore, brain histology in rats administered Cu alone revealed degenerated neurons and perforations in the cerebral cortical lamina. Interestingly, coadministration of Cu and rutin reduced the observed histological changes and improved inflammatory and antioxidant biomarkers, thus protecting against Cu-induced brain damage through antioxidant and anti-inflammatory mechanisms [36].

In these studies, copper sulfate caused oxidative stress in tissues. Rutin, resveratrol, and curcumin, with their antioxidant properties, reduced the oxidative stress caused by copper sulfate.

The study evaluated the effectiveness of Coenzyme Q10 (CoQ10) and its liposomal form (L-CoQ10) against CuSO4-induced myocardial damage, which is associated with toxic effects of excessive exposure to the pesticide copper sulfate (CuSO4). Copper sulfate increased the expression levels of cardiac MDA, TLR-4, NF-κB, IL-6, IL-1β, and TNF-α in the treatment groups. CoQ10 and L-CoQ10 prevented myocardial damage in the treatment groups, emphasizing that they may be important in protecting individuals vulnerable to Cu toxicity [39]. The results of this study are consistent with our study. Immunohistochemical analysis revealed increased NF-kB, TNF-κB, and IL-6 levels in the copper sulfate groups compared to the control group.

Real-time PCR analyses revealed that the relative mRNA expression of *TNFα*, *IL-6*, and *Nf-κB* genes in the lung, brain, kidney, liver, heart, and placenta tissues of rat fetuses exposed to Cu + + was presented as a fold change compared to the respective controls. TNFα was significantly increased in the brain and placenta; IL-6 in the brain, liver, heart, and placenta; and Nf-κB in the lung, heart, and placenta. Increased inflammation was also observed in these tissues compared to the control group. An increase in IL-6 has also been observed in the literature. Our results are consistent with previous studies [46].

No previous studies on double skeleton staining have been found in the literature. However, as in a previous study, a toxic effect was observed [25, 40]. Analyses revealed decreased bone development in the copper sulfate group compared to the control group. These data suggest that exposure to pesticides such as copper sulfate during pregnancy may harm fetal development.

Author contributions Sümeyye Uçar, Seher Yılmaz, Şükrü Ateş: They proposed the study and writing the manuscript and conducted the experimental study and data analysis. Aslı Okan Oflamaz, Züleyha Doğanyiğit, Osman Öztürk, and Evrim Suna Arıkan Söylemez: They conducted the data collection and analysis. All authors also read and approved the final manuscript.

Funding Open access funding provided by the Scientific and Technological Research Council of Türkiye (TÜBİTAK). The project was supported by Erciyes University Research Fund with THD-2024–13239 project.

Data availability No datasets were generated or analysed during the current study.

Declarations

Conflict of interest The authors declare that they have no financial conflicts of interest or personal relationships.

Ethical approval During this study, the conformity of the applications on animals to animal rights and animal experiments was approved by

the decision of Erciyes University, Experimental Animal Local Ethics Committee, dated 02.08.2023 and numbered 23/138.

Open Access This article is licensed under a Creative Commons Attribution 4.0 International License, which permits use, sharing, adaptation, distribution and reproduction in any medium or format, as long as you give appropriate credit to the original author(s) and the source, provide a link to the Creative Commons licence, and indicate if changes were made. The images or other third party material in this article are included in the article's Creative Commons licence, unless indicated otherwise in a credit line to the material. If material is not included in the article's Creative Commons licence and your intended use is not permitted by statutory regulation or exceeds the permitted use, you will need to obtain permission directly from the copyright holder. To view a copy of this licence, visit http://creativecommons.org/licenses/by/4.0/.

References

1. Araya M, Pizarro F, Olivares M, Arredondo M, González M, Méndez M. Understanding copper homeostasis in humans and copper effects on health. Biol Res. 2006;39(1):183–7.
2. Bost M, Houdart S, Oberli M, Kalonji E, Huneau JF, Margaritis I. Dietary copper and human health: current evidence and unresolved issues. J Trace Elem Med Biol. 2016;35:107–15.
3. Shanbhag VC, Gudekar N, Jasmer K, Papageorgiou C, Singh K, Petris MJ. Copper metabolism as a unique vulnerability in cancer. Biochim Biophys Acta Mol Cell Res. 2021;1868(2):118893.
4. Rocha GHO, Lini RS, Barbosa F, Batista BL, de Oliveira Souza VC, Nerilo SB. Exposure to heavy metals due to pesticide use by vineyard farmers. Int Arch Occup Environ Health. 2015;88(7):875–80.
5. Liu J, Lü X, Xie J, Chu Y, Sun C, Wang Q. Adsorption of lambda-cyhalothrin and cypermethrin on two typical Chinese soils as affected by copper. Environ Sci Pollut Res Int Haziran. 2009;16(4):414–22.
6. Genchi G, Catalano A, Carocci A, Sinicropi MS, Lauria G. Copper, cuproptosis, and neurodegenerative diseases. Int J Mol Sci. 2025;26(18):9173.
7. Kumar V, Kalita J, Bora HK, Misra UK. Relationship of antioxidant and oxidative stress markers in different organs following copper toxicity in a rat model. Toxicol Appl Pharmacol. 2016;293:37–43.
8. Raschke S, Ebert F, Kipp AP, Kopp JF, Schwerdtle T. Selenium homeostasis in human brain cells: Effects of copper (II) and Se species. J Trace Elem Med Biol. 2023;78:127149.
9. Chen L, Min J, Wang F. Copper homeostasis and cuproptosis in health and disease. Signal Transduct Target Ther. 2022;7:378.
10 Ala A, Walker AP, Ashkan K, Dooley JS, Schilsky ML. Wilson's disease. The Lancet. 2007;369(9559):397–408.
11. Hanağası F, Hanağası HA. Wilson Hastalığı. Türk Nöroloji Dergisi. 2013;19(4):122–7.
12 Kumar V, Kalita J, Bora HK, Misra UK. Temporal kinetics of organ damage in copper toxicity: A histopathological correlation in rat model. Regul Toxicol Pharmacol. 2016;81:372–80.
13 Babaei H, Kheirandish R, Ebrahimi L. The effects of copper toxicity on histopathological and morphometrical changes of the rat testes. Asian Pac J Trop Biomed. 2012;2(3):S1615–9.
14 Kalita J, Kumar V, Misra UK, Bora HK. Memory and learning dysfunction following copper toxicity: biochemical and ımmunohistochemical basis. Mol Neurobiol. 2018;55(5):3800–11.
15. Wan F, Zhong G, Ning Z, Liao J, Yu W, Wang C. Long-term exposure to copper induces autophagy and apoptosis through oxidative stress in rat kidneys. Ecotoxicol Environ Saf. 2020;190:110158.
16. Liu JY, Yang X, Sun XD, Zhuang CC, Xu FB, Li YF. Suppressive effects of copper sulfate accumulation on the spermatogenesis of rats. Biol Trace Elem Res. 2016;174(2):356–61.
17. Doğanyiğit Z, Okan A, Kaymak E, Pandır D, Silici S. Investigation of protective effects of apilarnil against lipopolysaccharide induced liver injury in rats via TLR 4/ HMGB-1/ NF-κB pathway. Biomed Pharmacother Mayıs. 2020;125:109967.
18. Inandiklioglu N, Doganyigit Z, Okan A, Kaymak E, Silici S. Nephroprotective effect of apilarnil in lipopolysaccharide-induced sepsis through TLR4/NF-κB signaling pathway. Life Sci. 2021;284:119875.
19 Liu J, Li J, Tian P, Guli B, Weng G, Li L. H2S attenuates sepsis-induced cardiac dysfunction via a PI3K/Akt-dependent mechanism. Exp Ther Med. 2019;17(5):4064–72.
20. Okan A, Doğanyiğit Z, Eroğlu E, Akyüz E, Demir N. Immunoreactive definition of TNF- α, HIF-1 α, Kir6.2, Kir3.1 and M2 muscarinic receptor for cardiac and pancreatic tissues in a mouse model for type 1 diabetes. Life Sci. 2021;284:119886.
21. Passmore MR, Byrne L, Obonyo NG, See Hoe LE, Boon AC, Diab SD. Inflammation and lung injury in an ovine model of fluid resuscitated endotoxemic shock. Respir Res. 2018;19(1):231.
22. Al-Haid S, Elalfy M, Alsyaed E, Abouelmagd M, Al-Jazzar A, Al-Hizab FA. The adverse side effects of prenatal and postnatal rats' exposure to silver nanoparticles ınduced toxicity. Open Vet J. 2024;14(8):1999–2006.
23. Chen YC, Yeh YC, Lin YF, Hsu SY, Nacis JS, Hsu JW. Aspartame intake during pregnancy induces placental dysfunction through impaired mitochondrial function and biogenesis modulation. Placenta. 2024;158:285–92.
24. Okan A, Demir N, Sozen B. Unfolded protein response triggers differential apoptotic mechanisms in ovaries and early embryos exposed to maternal type 1 diabetes. Sci Rep. 2021;11(1):12759.
25 Öztürk O, Uçar S, Doğanyiğit Z, Oflamaz AO, Arıkan ES, Ateş Ş. Evaluation of bone development and organs in rat fetuses exposed to tartrazine. Heliyon. 2025;11(1):e41456.
26 Iwashita Y, Zhang E, Maruyama J, Yokochi A, Yamada Y, Sawada H. Thrombomodulin protects against lung damage created by high level of oxygen with large tidal volume mechanical ventilation in rats. J Intens Care. 2014;2(1):57.
27. Kermanian F, Soleimani M, Pourheydar B, Samzadeh-Kermani A, Mohammadzadeh F, Mehdizadeh M. Effects of adenosine A2a receptor agonist and antagonist on cerebellar nuclear factor-kB expression preceded by MDMA toxicity. Med J Islam Repub Iran. 2014;28:120.
28 Pfaffl MW, Horgan GW, Dempfle L. Relative expression software tool (REST©) for group-wise comparison and statistical analysis of relative expression results in real-time PCR. Nucleic Acids Res. 2002;30(9):e36.
29. Li Y. Copper homeostasis: emerging target for cancer treatment. IUBMB Life. 2020;72(9):1900–8.
30 Uriu-Adams JY, Keen CL. Copper, oxidative stress, and human health. Mol Aspects Med. 2005;26(4):268–98.
31. Luo J, Hao S, Zhao L, Shi F, Ye G, He C. Oral exposure of pregnant rats to copper nanoparticles caused nutritional imbalance and liver dysfunction in fetus. Ecotoxicol Environ Saf. 2020;206:111206.
32. Lee IC, Ko JW, Park SH, Shin NR, Shin IS, Moon C. Comparative toxicity and biodistribution assessments in rats following subchronic oral exposure to copper nanoparticles and microparticles. Part Fibre Toxicol. 2016;13:56.
33. Liposomal Curcumin Attenuates the Incidence of Oxidative Stress, Inflammation, and DNA Damage Induced by Copper Sulfate in Rat Liver [Internet]. [a.yer 30 Eylül 2025]. Erişim

adresi: https://journals.sagepub.com/doi/epub/https://doi.org/10.1177/1559325818790869
34 Tian Y, Wu B, Li X, Jin X, Zhang F, Jiang C. The resveratrol alleviates the hepatic toxicity of CuSO4 in the rat. Biol Trace Elem Res. 2019;187(2):464–71.
35 Kalita J, Kumar V, Misra UK, Bora HK. Movement disorder in copper toxicity rat model: role of ınflammation and apoptosis in the *Corpus Striatum*. Neurotox Res. 2020;37(4):904–12.
36. Arowoogun J, Akanni OO, Adefisan AO, Owumi SE, Tijani AS, Adaramoye OA. Rutin ameliorates copper sulfate-induced brain damage via antioxidative and anti-inflammatory activities in rats. [a.yer 30 Eylül 2025]; Erişim adresi: https://doi.org/10.1002/jbt.22623
37. Yu W, Liao J, Yang F, Zhang H, Chang X, Yang Y. Chronic tribasic copper chloride exposure induces rat liver damage by disrupting the mitophagy and apoptosis pathways. Ecotoxicol Environ Saf. 2021;212:111968.
38 Erfanizadeh M, Noorafshan A, Naseh M, Karbalay-Doust S. The effects of copper sulfate on the structure and function of the rat cerebellum: a stereological and behavioral study. IBRO Neurosci Rep. 2021;11:119–27.
39. Alghibiwi HK, Alhusiani AM, Sarawi WS, Fadda L, Alomar HA, Alsaab JS. Coenzyme Q10 and its liposomal form prevent copper cardiotoxicity by attenuating oxidative stress, TLR-4/NF-κB signaling and necroptosis in rats. Cell Mol Biol. 2025;71(1):118–24.
40. Öztürk O, Dikici Y, Gür Ö, Ocak M, Doğanyiğit Z, Okan A. Evaluation of the effect of tartrazine on the offspring rats in an in vivo experimental model. Food Sci Nutr. 2024;12(11):9162–74.
41. Ozcelik D, Uzun H. Copper intoxication; antioxidant defenses and oxidative damage in rat brain. Biol Trace Elem Res. 2009;127(1):45–52. https://doi.org/10.1007/s12011-008-8219-3.
42. Okan A, Doğanyiğit Z, Yilmaz S, Uçar S, Arikan Söylemez ES, Attar R. Evaluation of the protective role of resveratrol against sepsis caused by LPS via TLR4/NF-κB/TNF-α signaling pathways: experimental study. Cell Biochem Funct. 2023;41(4):423–33. https://doi.org/10.1002/cbf.3790.
43. Guo H, Ouyang Y, Yin H, et al. Induction of autophagy via the ROS-dependent AMPK-mTOR pathway protects copper-induced spermatogenesis disorder. Redox Biol. 2022;49:102227. https://doi.org/10.1016/j.redox.2021.102227.
44. Ma Q, Ying M, Sui X, et al. Chronic copper exposure causes spatial memory impairment, selective loss of hippocampal synaptic proteins, and activation of PKR/eIF2α pathway in mice. J Alzheimers Dis. 2015;43(4):1413–27. https://doi.org/10.3233/JAD-140216.
45. Wu H, Guo H, Liu H, et al. Copper sulfate-induced endoplasmic reticulum stress promotes hepatic apoptosis by activating CHOP, JNK and caspase-12 signaling pathways. Ecotoxicol Environ Saf. 2020;191:110236. https://doi.org/10.1016/j.ecoenv.2020.110236.
46 Farag WG, El-Kossi DMMH, Nafadi EKM. Biological effects of D-penicillamine on copper sulfate-induced possible damage in the caudate nucleus: role of apoptotic genes Bax, Bcl2, and Bax-Bcl2 ratio. Biol Trace Elem Res. 2025. https://doi.org/10.1007/s12011-025-04847-z.

Publisher's Note Springer Nature remains neutral with regard to jurisdictional claims in published maps and institutional affiliations.